The 4th International Conference for Conveying and Handling of Particulate Solids
Budapest, Hungary, May 2003

WAVELET MULTI-RESOLUTION CROSS-CORRELATION ANALYSIS OF SWIRLING GAS-SOLID FLOW IN A HORIZONTAL PIPE

H. Li[1], M. Takei[2], Y. Tomita[3], Y. Saito[4] and K. Horii[5]
1. Department of Mechanical Engineering, Kagoshima University
1-21-40, Korimoto, Kagoshima 890-0065, JAPAN
2. Department of Mechanical Engineering, Nihon University
1-8-14, Kanda Surugadai, Chiyoda-ku, Tokyo, JAPAN
3. Department of Mechanical Engineering, Kyushu Institute of Technology
1-1, Sensuicho, Tobata Kitakyushu, JAPAN
4. Department of Electrical & Electonic Engineering, Hosei University
3-7-2, Kajino, Koganei, Tokyo, JAPAN
5. Shirayuri Women's College
1-25 Modorigaoka, Chofu-shi, Tokyo, JAPAN

Abstract – The wavelet multiresolution cross-correlation analysis were developed and applied to experimental pressure-time signals, in order to analyze the characteristics of swirling gas-solid flow in both Fourier and physical spaces. It was revealed that dunes with same moving velocity of 1 m/s pass through test pipeline and non-correlation existed at smaller scales that represent heterogeneous suspension flow over the dunes.

1. INTRODUCTION

Pneumatic conveying is an important operation in a significant number of industrial processes, such as the transportation of materials from storage areas, in catalytic cracking in the petroleum industry, and in the production of synthetic fuels from coal in energy conversion systems. Conventional pneumatic conveying, that is axial flow pneumatic conveying, is frequently operated in the dilute-phase regime in the high air velocity region. Power consumption, pipe erosion, and particle degradation considerations dictate that the conveying velocity be held to a minimum. In the last thirty-five years, there has been increasing interest in dense-phase pneumatic conveying, and several commercial systems have been developed. Unfortunately, these systems require high pressure drops and have high initial costs. Furthermore, dense-phase pneumatic conveying may lead to unstable flows at low conveying velocities. These unstable flows often cause blockage and pipe vibration.

To reduce power consumption, blockage, particle degradation and pipe wear, this new swirling flow technique, called swirling flow pneumatic conveying, was applied to horizontal and vertical pneumatic conveying by Li and Tomita (1996, 1998) [1], [2]. In the low velocity conveying range, SFPC was determined to be effective.

However, swirling gas-solid flow is unsteady and complicated nonlinear dynamics system. A detailed understanding of the behavior of particles is importance for design, optimization and operation of swirling flow pneumatic conveying system. Although identification of visual flow patterns may be adequate for some cases [1], [2], in many situations these methods are not applicable or are too subjective. Several other methods have been developed to more objectively identify and interpret flow patterns and transitions of two-phase flow, such as pressure signal analysis, root mean square of pressure-time series, correlation function, skewness and flatness factor, the power spectral density function and probability density function [3]-[6]. These studies have contributed to our understanding of flow patterns and transitions of two-phase flow in statistics, It is well known that pressure signals contain sufficient information on peculiar features of flow pattern and unsteady characteristics of pneumatic conveying. However, the convenctional techniques lost the information on the time for obtaining statistical characters.

The aim of this paper is to develop an application of wavelet technique to the swirling gas-solid flow. The wavelet multiresolution cross-correlation analysis approach is applied to the experimental data of pressure-time signals in a horizontal swirling gas-solid flow for extracting the most essential scales governing the correlation features.

2. WAVELET MULTI-RESOLUTION ANALYSIS

The discrete wavelet transform is a linear and orthogonal transform. Generally, for an one-dimensional data matrix $\boldsymbol{V}$,

$$V = \begin{bmatrix} v_1 & v_2 & . & . & . & v_N \end{bmatrix}^T \tag{1}$$

the discrete wavelet transform can be defined in matrix form as

$$\boldsymbol{S}=\boldsymbol{WV} \tag{2}$$

where $\boldsymbol{S}$ and $\boldsymbol{W}$ is called discrete wavelet coefficient (or spectrum) matrix of $\boldsymbol{V}$ and the analysing wavelets matrix, respectively, the superscript ^{T} represents the transpose matrix. The analysing wavelets matrix is an orthogonal and satisfies $\boldsymbol{W}^T\boldsymbol{W}=\boldsymbol{I}$, where $\boldsymbol{I}$ is a unit matrix. The analysing wavelets matrix is usually constructed based on a cascade algorithm of an orthogonal wavelet basis function. The Haar function is perhaps the first orthogonal wavelet basis, which was constructed even long before the term "wavelet" was invented. In the last decade, various orthogonal wavelet bases have been constructed, including Meyer basis, Daubechies basis, Coifman basis, Battle-Lemarie basis, Baylkin basis, spline basis, which provide excellent localization properties in both physical and Fourier spaces. Different wavelet basis functions will preferentially move, between scales, different characteristics of the target data sets. Such as, use of Harr basis function may emphasize discontinuous in the target data sets, and the Daubechies family may emphasize the smoothness of the analysed data. Here, we use the Daubechies wavelet with orders 4, which has only four coefficients, c_0, c_1, c_2 and c_3, to explain how to construct the analysing wavelets matrix and the processing of discrete wavelet transform. It is no lack of generality to use Daubechies wavelet with orders 4 for illustrating the discrete wavelet transform. Daubechies wavelet with orders 4 may be expressed by the following matrix.

$$\begin{bmatrix}
c_0 & c_1 & c_2 & c_3 & & & & & & & \\
c_3 & -c_2 & c_1 & -c_0 & & & & & & & \\
 & & c_0 & c_1 & c_2 & c_3 & & & & & \\
 & & c_3 & -c_2 & c_1 & -c_0 & & & & & \\
\cdot & \cdot & & & \cdot & & & & & & \\
\cdot & \cdot & & & & \cdot & & & & & \\
\cdot & \cdot & & & & & \cdot & & & & \\
 & & & & & & c_0 & c_1 & c_2 & c_3 \\
 & & & & & & c_3 & -c_2 & c_1 & -c_0 \\
c_2 & c_3 & & & & & & & c_0 & c_1 \\
c_1 & -c_0 & & & & & & & c_3 & -c_2
\end{bmatrix}, \tag{3}$$

where blank entries signify zeroes. The action of the matrix, overall, is thus to perform two related convolutions, then to decimate each of them by half and interleave the remaining halves. It is useful to think of the coefficients c_0, c_1, c_2 and c_3 as being a smoothing filter, something like a moving weight average of four points. Then because of the minus signs, the coefficients c_3, $-c_2$, c_1 and $-c_0$ is not a smoothing filter, something like a moving weight difference filter. The discrete wavelet transform consists of applying the wavelet basis like the Daubechies wavelet with orders 4 *hierarchically*, first to the full data matrix of length N (N must be a higher power of two), then to the "smooth" elements of length $N/2$, then to the "smooth-smooth" elements of $N/4$, and so on until only a trivial number of "smooth-...-smooth" elements (usually 2) remain. After each smooth processing, the smoothed elements are permuted to the first $i/2$ position of the matrix and the non-smoothed elements are permuted to the next $i/2$ position of the matrix by premultiplying a matrix $\boldsymbol{P}^{(i)}$, where i is N, $N/2$, $N/4$, ..., 4, and also indicate the number of non-zero row in matrix $\boldsymbol{P}^{(i)}$. The procedure is sometimes called a *pyramidal algorithm*. In this *pyramidal* processing the analysing wavelets matrix is obtained by

$$\boldsymbol{W}=\boldsymbol{P}^{(4)}\boldsymbol{C}^{(4)}\ldots\boldsymbol{P}^{(N/2)}\boldsymbol{C}^{(N/2)}\boldsymbol{P}^{(N)}\boldsymbol{C}^{(N)} \tag{4}$$

where matrix $\boldsymbol{P}^{(i)}$ ($i = N$ to 4) is a permuting matrix. In this study, the Daubechies wavelet with orders 20 is used as the orthonormal wavelets instead of Daubechies wavelet with orders 4, since a high order wavelet base has good frequency localization that in turn increases the energy compaction. Since the analysing wavelets matrix and wavelet basis are orthogonal functions, the discrete wavelet transform has the inverse transform. One simply reverses the procedure, starting with the smallest level of the hierarch and working from right to left, and the inverse discrete wavelet transform can be simply carried out by

$$\boldsymbol{V}=\boldsymbol{W}^T\boldsymbol{S}. \tag{5}$$

The discrete wavelet coefficient is usually interpreted as the relative local contribution of various scales to the original data instead of the original data components of each scale. In order to decompose the data into the grouped frequency components, the inverse wavelet transform is applied to the discrete wavelet coefficients at each grouped frequency. This decomposition method is called the wavelet multi-resolution analysis. Hence, Eq. (5) can be rewritten by

$$V=\sum_{i=1}^{n} W^T S_i\,. \tag{6}$$

On the right side of the above Eq. (6), the first term $\boldsymbol{W}^T\boldsymbol{S}_1$ and the last term $\boldsymbol{W}^T\boldsymbol{S}_n$ represent the data components at wavelet level *1* (the lowest frequency) and level n (the highest frequency).

3. EXPERIMENTAL APPARATUS AND PROCEDURE

In this study the experimental facility is the pressurized system and is shown schematically in Fig.1. Air from a blower flows through the calibrated nozzle and a vaned swirler in the stabilizer pipe, and picks up the solid materials fed by gravity from the feed tank at the inlet of conveying pipeline. Then, the solids-air mixture enters the conveying pipeline and at the pipeline exit the solids are separated from the solids-air mixture by the separator. The conveying pipeline consisted of a horizontal smooth acrylic tube of 76 mm inside diameter and about 7.5 m length.

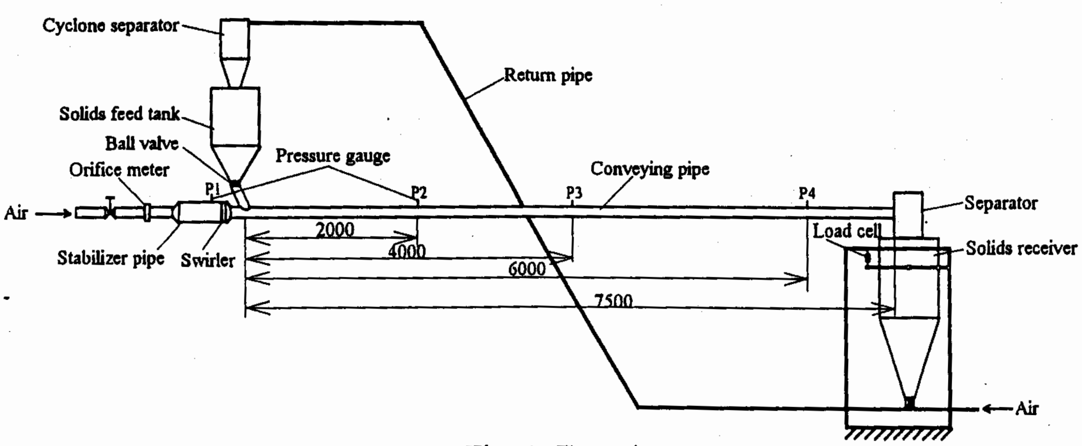

Fig. 1: Experimental setup

The airflow rate was measured by the orifice meter, and the fluctuation of solid mass flow rate was measured by a load cell. The fluctuations of static pressure along the pipeline were measured at locations L=2, 4 and 6 m from the solid feed point by use of semiconductor pressure transducers, whose frequency response is 800 Hz. The data length of 8000 points for each test case was utilized to carry the wavelet analysis. Polyethylene pellets of 3.5 mm and a density of 1210 kg/m^3 were used as test solids. The mean air velocity U_a was from 6 to 28 m/s and the solid mass flow rate G_s from 0.3 to 0.5 kg/s. The initial swirl number S_0, which was defined at the inlet of conveying pipeline and calculated using author's method (Li and Tomita 1994) [7], was varied from 0.00-0.61.

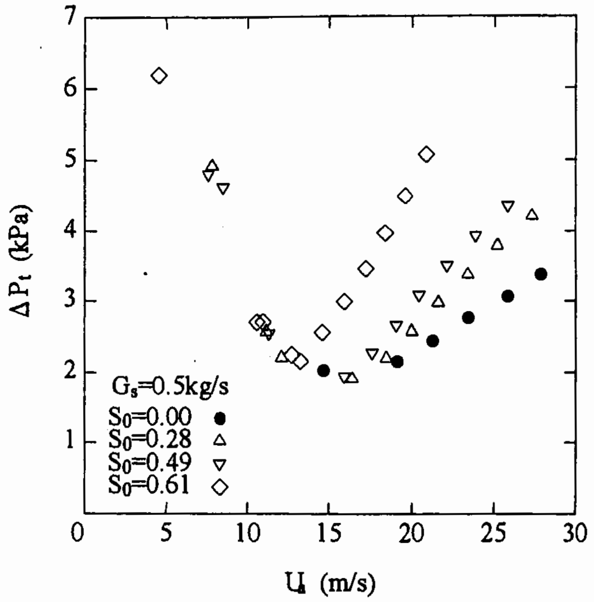

Fig. 2: Relation between the total pressure drop and air velocity

4. RESULTS AND DISCUSSION

4.1 Total Pressure Drop

The same as the previous paper [1], the total pressure drop Δp_t contains the pressure drop due to the vaned swirler, i.e., the total pressure drop between the stabilizer pipe and the exit of conveying pipe is considered. For steady state flow, Δp_t can be obtained as follows:

$$\Delta p_t = \Delta p_1 - \frac{1}{2}\rho_a\left[1-\left(\frac{D}{D_0}\right)^4\right]U_a^2, \tag{7}$$

where Δp_1 is the wall static pressure of stabilizer pipe before the vaned swirler, D and D_0 are the diameters of pipeline and stabilizer pipe, respectively.

Figure 2 shows the total pressure drop versus the air velocity with the initial swirl number S_0 as a parameter for the solids mass flow rate 0.5*kg/s*. According to S_0, three kinds of swirling gas-solid flow are called swirl 1 flow (S_0=0.28), swirl 2 flow (S_0=0.49) and swirl 3 flow (S_0=0.61), respectively. From Fig.2 it is evident that the minimum and critical velocity of swirling gas-solid flow are smaller than that of non-swirling gas-solid flow. The same as non-swirling gas-solid flow the pressure drop of swirling gas-solid flow firstly decreases and then rises below the minimum velocity, when air velocity decreases. Comparing swirling with non-swirling gas-solid flow in Fig.2, the pressure drop of swirling gas-solid flow is higher than that of non-swirling gas-solid flow in range of high air velocity. However, below and near the minimum velocity of swirling gas-solid flow, the pressure drops of swirl 1 and swirl 2 flow become lower than that of non-swirling gas-solid flow. On the other hand, swirl 1, swirl 2 and swirl 3 flow show same pressure drop in range of low air velocity due to the weak swirl flow.

4.2 Wavelet Multiresolution Cross-Correlation Analysis of Pressure Fluctuations

In identifying the spatial structure of signals and its evolution in time, the cross-correlation analysis between two signals is most used. A difficulty with the conventional cross-correlation method, however, is that the cross-correlation function only provides information about the cross-correlation behavior in terms of time delay but no information about correlation behaviors in scale space due to lack of scale resolution. Recently, Li (1998) [8] developed wavelet cross-correlation analysis based on the continuous wavelet transform. The wavelet cross-correlation analysis provides the unique capability for decomposing the correlation of arbitrary signals over a two-dimensional time delay-period plane. In analogy with the wavelet cross-correlation, in this study we first unfold respectively two different signals into their two-dimensional time-scale planes using wavelet multiresolution analysis. Then we use two signal components coming from different signals with same wavelet level to define a cross-correlation function, called the *wavelet multiresolution cross-correlation function.* In analogy with the traditional cross-correlation method, we adopt the *wavelet multiresolution cross-correlation coefficients* R_w in this paper.

Since swirling flow gas-solid flow has been determined to be effective in the low velocity range, we attempt to analyze the feature of dune flow pattern of particles in the present work. Figure 3(a) shows the wavelet multiresolution cross-correlation coefficients of wall fluctuating pressures between the location x = 2 m and 4 m for U_a = 8.66 m/s, G_s = 0.3 kg/s and S_0 = 0.61. The conventional cross-correlation coefficients are also included. It is evident that the distribution of conventional cross-correlation coefficients is similar to wavelet multiresolution cross-correlation coefficients of level 1, however, its amplitude is smaller than that of wavelet multiresolution cross-correlation coefficients and cannot provide cross-correlation information at other scale. The wavelet multiresolution cross-correlation coefficients describe this fact that the cross-correlation becomes weaker as the wavelet level increases or scale decreases. The stronger correlation exists at level 1 and 2, and implies periodic motion of dune within these two scale ranges. The moving velocities of dunes may be calculated based on wavelet multiresolution cross-correlation, and give 1*m/s* and 2*m/s*, respectively.

The wavelet multiresolution cross-correlation coefficients of wall fluctuating pressures between the location x = 4 and 6 m is shown in Fig.3 (b). The conventional cross-correlation coefficients become smaller than that of Fig.3 (a). The wavelet multiresolution cross-correlation coefficients of level 1 remain the larger correlation, and the moving velocities of dunes computed from distribution of peaks are same as Fig.3 (a). This indicates that the dunes with same moving velocity pass through the test pipeline. The wavelet multiresolution cross-correlation of level 2 becomes weaker. Although stronger peaks are observed in the fluctuating pressure components of level 8 (no shown), which represent heterogeneous suspension flow over the dunes, the non-correlation is found at level 8. This may be interpreted as the random motion of particles.

It is clear that the wavelet multiresolution cross-correlation analysis can provide the information on correlation at various scales, and extract the most essential scales governing the correlation features, which is difficulty if using conventional method.

5. CONCLUSIONS

(1) The wavelet multiresolution cross-correlation analysis can provide the information on correlation between two different signals at various scales, and reveals that dunes with same moving velocity of 1 m/s pass through test pipeline.

(2) Non-correlation was found at smaller scales that represent heterogeneous suspension flow over the dunes.

REFERENCES

1. H. Li and Y. Tomita, An Experimental Study of Swirling Flow Pneumatic Conveying System in a Horizontal Pipeline, *ASME Journal of Fluid Engineering* **118**, pp.526-530, 1996.
2. H. Li and Y. Tomita, An Experimental Study of Swirling Flow Pneumatic Conveying System in a Vertical Pipeline, *ASME Journal of Fluids Engineering* **120**, pp.200-203, 1998.
3. M. Takei, M. Ochi, K. Horii, H. Li and Y. Saito, Discrete Wavelets Auto-correlation of Axial Turbulence velocity in Spiral Single Phase Flow, *Powder Technology* **112**, pp.289-298, 2000.
4. H. Li and Y. Tomita, Characterization of Pressure Fluctuation in Swirling Gas-Solid Two-Phase Flow in a Horizontal Pipe, *Advanced Powder Technology* **12**, pp.169-186, 2001.
5. Y. Tsuji and Y. Morikawa, Flow Pattern and Pressure Fluctuation in Air-Solid Two-Phase Flow in a Pipe at Low Air Velocities, *Int. J. Multiphase Flow* **8**, 329-341, 1982.
6. S. Matsumoto and H. Harakawa, Statistical Analysis of the Transition of the Flow Pattern in Vertical Pneumatic Conveying, *Int. J. Multiphase Flow* **13**, 123-129, 1987.

7. H. Li and Y. Tomita, Characteristics of Swirling Flow in a Circular Pipe, *ASME Journal of Fluid Engineering* **116**, 370-373, 1994.
8. H. Li, Identification of Coherent Structure in Turbulent Shear Flow with Wavelet Correlation Analysis, *ASME Journal of Fluids Engineering* **120**, 778-785, 1998.

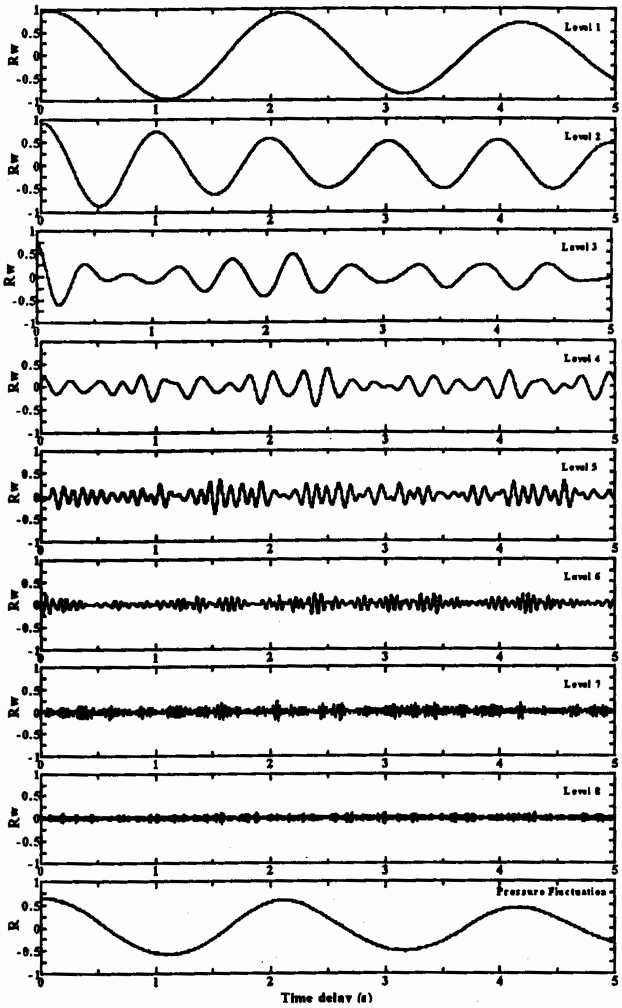

Fig. 3 (a): Multiresolution cross-correlation of fluctuating pressures between the location x=2m and 4m (U_a=8.66m/s, G_s=0.3kg/s and S_0=0.61)

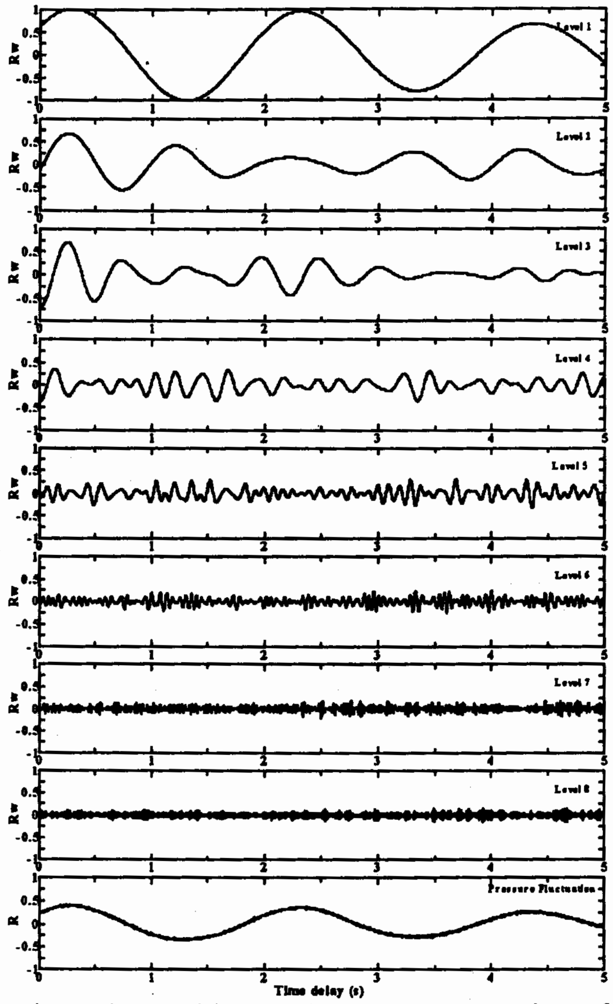

Fig. 3 (b): Multiresolution cross-correlation of fluctuating pressures between the location x=4m and 6m (U_a=8.66m/s, G_s=0.3kg/s and S_0=0.61)